COMBINED USE OF PHOTOELECTRIC AND LASER-HETERODYNE TECHNIQUES TO MEASURE SOUND VELOCITIES IN SHOCK-COMPRESSED METALS

E.A. Kozlov, D.G. Pankratov, D.P. Kuchko, A.K. Yakunin, A.G. Poptsov, M.A. Ralnikov

RFNC-VNIITF, Snezhinsk, Russia

Using investigation into stepped samples out of austenitic steel 12Kh18N10T and high-purity magnesium of Mg95 grade, under shock-wave loading in the range $\sigma_{xx} = 60…120$ GPa and 20…30 GPA, respectively, the efficiency of combination of photoelectric (PET) and laser-heterodyne (PDV) techniques was demonstrated in each explosive experiment.

The combination of techniques expanded the range of application and improved the reliability of obtained self-consistent information on the sound velocities in shock-compressed structural and model materials.

Introduction

Interest in determining longitudinal c_l and bulk c_b sound velocities in shock-compressed matter is explained by the fact that they are primary values in many processes related to shock waves (SW) and rarefaction waves (RW). Measurements of longitudinal $c_l(\sigma_{xx})$ and bulk $c_b(\sigma_{xx})$ sound velocities in shock-compressed materials permit to get information about their plasto-elastic properties. Besides, as far as elastic moduli of various phases of one and the same material drastically differ, by sudden change of dependences $c_l(\sigma_{xx})$ и $c_b(\sigma_{xx})$, one can judge about the change of phase composition of material along its shock adiabat and refine the coordinates of shock adiabat crossing with the boundaries of phase equilibriums in p,T-plane [5].

In order to determine c_l and c_b, we use method of overtaking unloading – registration of the moments of rarefaction waves head characteristics arrival that leads to the change of registered parameters of flow, which is in the contact with the sample under study for PET of either samples contact boundary velocity and window material, or sample free surface velocity for PDV.

The goal of work is to demonstrate the efficiency of combining PET and PDV while performing the measurements of sound velocities for several structural and model materials.

Material, samples, indicators and conditions of their explosive loading

This work investigated: stainless steel 12Kh18N10T and magnesium of Mg95 grade. For indicators, chloform ($CHCl_3$) and carbogal (C_8F_{16}) were used. While making calculation assessments of the parameters of the states of investigated processes, the following D,u–ratios were used:

- for steel 12Kh18N10T ($\rho_0 = 7.89$ g/cm^3) – $D = 4.56 + 1.501u$, $u < 3$ km/s [11];
- for magnesium Mg95 ($\rho_0 = 1.74$ g/cm^3) – $D = 4.54 + 1.238u$, $u < 7.4$ km/s [12];
- for chloroform $CHCl_3$ ($\rho_0 = 1.483$ g/cm^3) – $D = 1.317 + 1.572u$, $0{,}8 < u < 2.9$ km/s [13];
- for carbogal C_8F_{16} ($\rho_0 = 1.858$ g/cm^3) – $D = 0.9 + 2u - 0.0622u^2$, $0 < u < 3$ km/s [14].

The samples were discs, which had four steps of sector form (Figure 1). The step thickness h was selected by the results of calculation-theoretical assessments of investigated processes that were made before explosive experiments. While selecting the step height, we excluded the influence of lateral unloading waves from the sample edges and cumulative jets, which are the aftereffects of the sample stepped shape, on the results of measurements.

Explosive loading of the samples was performed using small-size devices (SLD) with HE charges ∅60 mm in diameter, with energy release up to 300 g TNT. The flat front of detonation wave at SLD output was formed with the help of explosive lens. The main parameters of the charges are shown in the

Table1. Figure 1 shows a sketch of experimental node (no scale). Table 2 shows calculation parameters of the states realized in experiments.

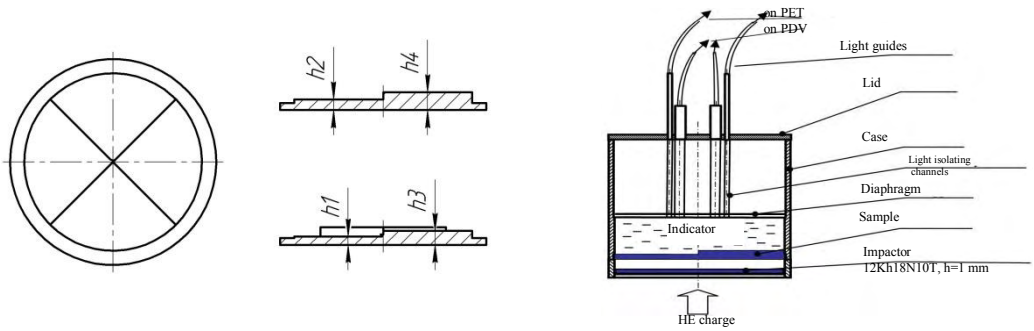

Figure 1. Design of four-step sample and sketch of experimental node (no scale)

Table 1. SLD main parameters

№	HE type	HE thickness, mm	Impactor material	H_{im}, mm	W_{im}, km/s	Flight range, mm
1	Mixture TNT-RDX	-	12Kh18N10T	1	2.31	6
2	Mixture TNT-RDX	5	12Kh18N10T	1	2.59	6
3	Mixture TNT-RDX	10	12Kh18N10T	1	2.84	6
4	HMX-based composition	10	12Kh18N10T	1	3.12	6
5	HMX-based composition	15	12Kh18N10T	1	3.47	7
6	HMX-based composition	25	12Kh18N10T	1	3.96	9

Table 2. Calculation parameters of states

SLD #	2	4	5	6		1	3
Impactor	12Kh18N10T						
ρ_0, g/cm^3	7.89						
W_{im}, km/s	2.59	3.12	3.47	3.96		2.31	2.84
Sample	12Kh18N10T					Mg95	
ρ_0, g/cm^3	7.89					1.73	
D_{sam}, km/s	6.50	6.90	7.16	7.53		6.77	7.27
U_{sam}, km/s	1.29	1.56	1.74	1.98		1.80	2.20
$\sigma_{xx\ sam}$, GPa	66.4	84.9	98.0	117.7		21.3	27.8
ϱ, g/cm^3	9.85	10.19	10.41	10.70		2.36	2.48
c_l, km/s*	7.80	8.16	8.39	8.69		7.52	7.85
Indicator	C_8F_{16}					$CHCl_3$	
ρ_0, g/cm^3	1.86					1.483	
D_{ind}, km/s	4.87	5.54	5.97	6.55		4.76	5.43
U_{ind}, km/s	2.13	2.52	2.77	3.13		2.19	2.61
P_{ind}, GPa	19.2	25.9	30.8	38.1		15.5	21.0

* - for c_l assessment in steel 12Kh18N10T, dependence $c_l = 1.047\varrho - 2.515$ [3] was used;
for c_l assessment in Mg95, the results of work [15] were used.

The results of experiments

In the frames of work, 6 experiments were made on registration of the processes of combined technique PET-PDV both on SW front in indicator liquid, and behind SW front in case, if liquid preserves its complete or partial transparency in shock waves of low or moderate intensity. In other words in the region of weak shock compressions, where it is difficult to get information by PET technique, necessary data will be obtained with the help of PDV. In the region of moderate and strong shock waves, both techniques register the dynamics of shock wave propagation over indicator matter and the moment, when shock wave is overtaken in the indicator of the first characteristic in elastic and plastic unloading fans. Such combined diagnostics is to permit to overcome contradictions in sound velocities measurements in some structural and model materials that were mentioned in papers [4, 16].

Ocsillograms that were obtained in the tests with registration of the processes by PET and the examples of spectrograms that were obtained in four PDV channels for each experiment are shown in Figures 2 and 3.

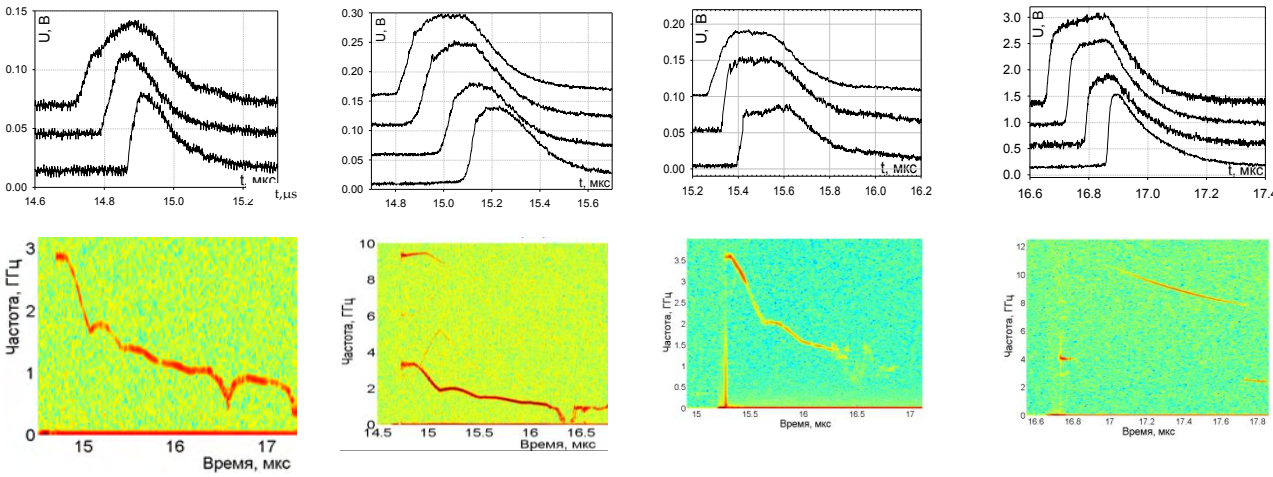

a) b) c) d)

a) test 115/1344 (K97); b) test 114/1344 (K96); c) test 141/1344 (K127); d) test 147/1344 (K137).

Figure 2. PET ocsillograms and PDV spectrograms obtained in tests.
Samplematerial – steel 12Kh18N10T, indicator –carbogal C_8F_{16}

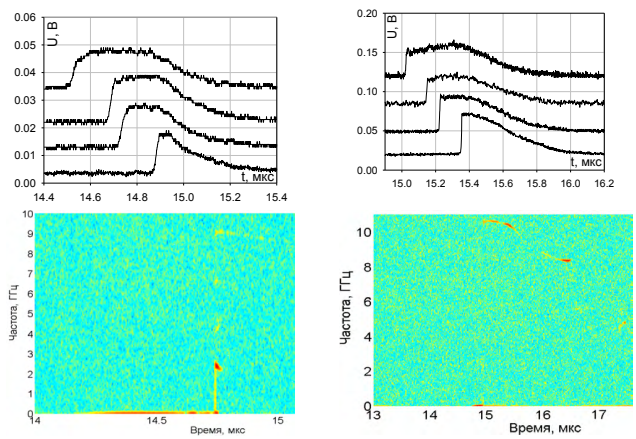

a) **b)**

a) test 125/1344 (K118); b) test 124/1344 (K117).

Figure 3. PET ocsillograms and PDV spectrograms obtained in tests.
Sample material – magnesium Mg95, indicator – chloroform $CHCl_3$

PET ocsillograms show that expected phenomena in the samples under study were registered. Ocsillograms layout is made for the first experiment. On the rest ocsillograms, described phenomena are similar. Time is measured from the moment of voltage application to electro detonator.

PDV spectrograms show that in all experiments, it was possible to register the profiles of velocity either of the boundary sample-indicator (Figure (a, в)), or SW front velocity in indicator (Figure 3(b)), or simultaneously both (Figure 2(b, d), Figure 3(a)). Time of PDV spectrograms is measured also from the moment of voltage application to electro detonator.

Data presented in Figures 2 and 3 show that in the region of low loadings, carbogal plays the role of a window material, preserving transparency in near IR-range. PDV registers time change of the motion of the interface sample-indicator through the layer of shock-compressed carbogal. At the same time, SW front luminescence in spectral range 0.30÷0.65 μm is rather stable, and this is confirmed by the quality of ocsillograms that were obtained with the help of PET. With increase of intensity of sample shock-wave loading, PDV begins to register the reflection of Doppler signal from SW front in carbogal. Stability of shock-compressed carbogal luminescence intensity in the range 0.30÷0.65 μm is improved, but carbogal still preserves transparency, and this is confirmed by PDV registration of the motion not only of SW front in carbogal, but of the motion of the boundary between the sample under study образца and carbogal.

Use of carbogal as indicator liquid in low pressure range has disadvantage, namely greater carbogal inertness in comparison with chloroform. This is confirmed by longer time of signal leading edge increment at comparable levels of shock loading.

For chloroform (Figure 3), quick loss of transparency is typical under small increase of loading pulse amplitude. In realized pressure range, chloroform is already opaque, that is why it was impossible to register the whole profile sample-indicator interface motion velocity. Perhaps, this will be feasible by decreasing loading pulse amplitude, i.e. using impactors flying at lower velocity. Even not registering the velocity of motion of interface "substance under study-indicator", PDV registers constantly the velocity of strong shock wave front motion in chloroform.

Qualitative ocsillogram and spectrogram processing

PET. The results of experimental-calculation determination of sound velocities in shock-compressed steel 12Kh18N10T and magnesium Mg95 are given in Tables 3 and 4. Graphic displaying of obtained results is shown in Figure 6. There are also the results of PDV measurements and the result of data approximation by sound velocities in steel 12Kh18N10T that were obtained at RFNC-VNIITF with the help of PET in the range of stresses 50 ÷ 200 GPa [3]. The dependence of sound velocity in steel on density was described by a single dependence $c_l = 1.047\rho - 2.515$ (Birch's Law [17]) and then recalculated in the dependence of sound velocity on longitudinal stress in the sample $c_l(\sigma_{xx})$. For magnesium, the graph shows the results of earlier made experiments at RFNC-VNIITF with the help of two techniques: manganin gauges method (MGM) and PET.

Error of sound velocity measurements by PET makes ±1,5% under "symmetric" impact (tests on steel) and ±3% under "nonsymmetric" one (tests on Mg95).

PDV. Velocity profiles reconstructed by spectrograms are shown in Figures 4 and 5. The results of experimental-calculation determination of sound velocities in shock-compressed steel 12Kh18N10T and мmagnesium Mg95 are shown in Tables 5 and 6.

Table 3. Longitudinal sound velocity in steel 12Kh18N10T according to PET measurements data

Test #	Loading device				Sample of12Kh18N10T		
	SLD #	Charge sizes	Impactor	W_{im}, km/s	$\sigma_{xx\ calculation}$, GPa	$c_{l\ calculation}$, km/s	$c_{l\ exp}$, km/s
115/1344	2	∅60×5	12Kh18N10T	2.59	66.4	7.80	**7.90±0.12**
114/1344	4	∅60×10		3.12	84.9	8.16	**8.06±0.12**
141/1344	5	∅60×15		3.47	98.0	8.39	**8.22±0.13**
147/1344	6	∅60×25		3.96	11.7	8.69	**8.78±0.13**

Table 4. Longitudinal sound velocity in magnesium Mg95 according to PET measurements data

Test #	Loading device				Mg95 sample		
	SLD #	Charge sizes	Impactor	W_{im}, km/s	$\sigma_{xx\ calculation}$, GPa	$c_{l\ calculation}$, km/s	$c_{l\ exp}$, km/s
125/1344	1	-	12Kh18N10T	2.31	2.2	7.52	**7.81±0.23**
124/1344	3	∅60×10		2.84	27.7	7.85	**7.90±0.23**

Graphic displaying of obtained results is shown in Figure 6. Error of c_l measurements by PDV makes ±1.6% under "symmetric" shock (tests on steel) and ±2.8% under "nonsymmetric" one (tests on Mg95). The results of c_l measurements in shock-compressed steel 12Kh18N10T (in the range 66-118 GPa) and in high-purity Mg (in the range 21-28 GPa) by two techniques are in good agreement. Accuracies of sound velocities measurements in shock-compressed materials are close, in PDV case, it is some higher, but its main advantage – its operability in wider range of pressures and shock compression temperatures.

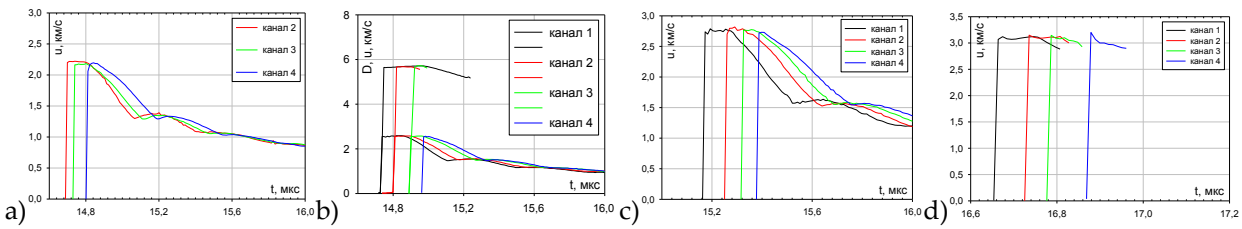

a) test 115/1344 (K97); b) test 114/1344 (K96) GPa; c) test 141/1344 (K127); d) test 147/1344 (K137).

Figure 4. Velocity profiles reconstructed by PDV spectrograms.
Sample material – steel 12Kh18N10T, indicator – carbogal C_8F_{16}

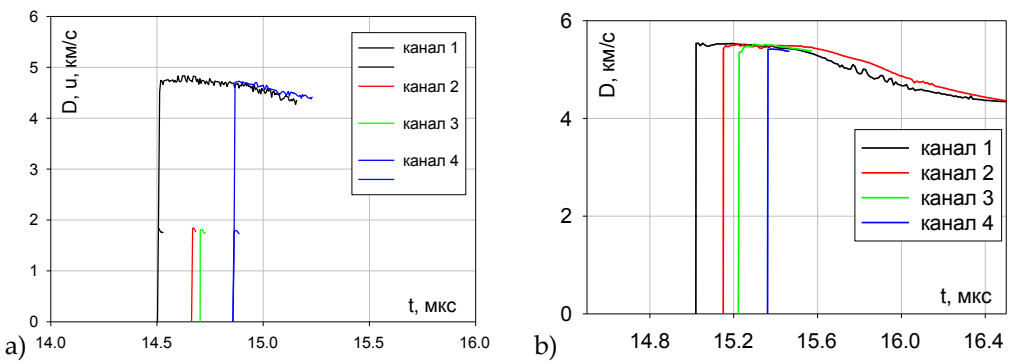

a) test 125/1344 (K118); b) test 124/1344 (K117).

Figure 5. Velocity profiles reconstructed by PDV spectrograms.
Sample material – magnesium Mg95 and indicator – chloroform $CHCl_3$

Table 5. Longitudinal sound velocity in steel 12Kh18N10T according to PDV measurements data

Test#	Loading device				Sample of 12Kh18N10T		
	SLD #	Charge sizes	Impactor material and thickness	W_{im}, km/s	$\sigma_{xx\ calculation}$, GPa	$C_{calculation\ l}$, km/s	$c_{l\ exp}$, km/s
115/1344	2	∅60×5	12X18H10T $h_{уд}$ = 1 мм	2.59	66.4	7.80	**7.93±0.13**
114/1344	4	∅60×10		3.12	84.9	8.16	**8.25±0.14**
141/1344	5	∅60×15		3.47	98.0	8.39	**8.46±0.14**
147/1344	6	∅60×25		3.96	117.7	8.69	**8.82±0.15**

Table 6. Longitudinal sound velocity in magnesium Mg95 according to PDV measurements data.

Test#	Loading device				Mg95 sample		
	SLD #	Charge sizes	Impactor material and thickness	W_{im}, km/s	$\sigma_{xx\ calculation}$, GPa	$c_{l\ calculation}$, km/s	$c_{l\ exp}$, km/s
125/1344	1	-	12X18H10T	2.31	21.2	7.52	**7.90±0.22**
124/1344	3	∅60×10	H_{im} = 1 мм	2.84	27.7	7.85	**7.98±0.22**

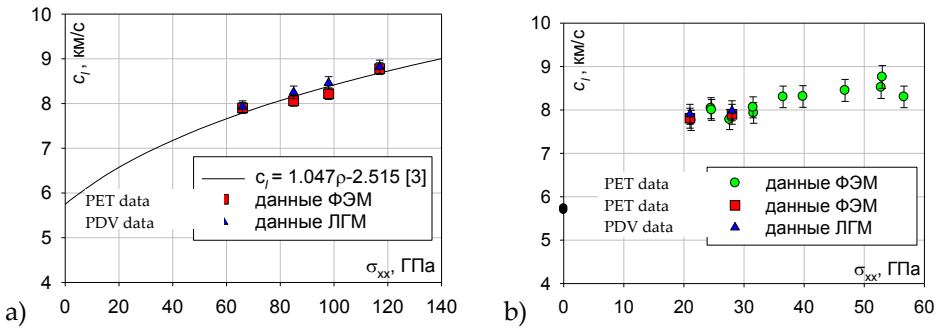

Figure 6. Comparison of the results on sound velocities obtained by PET and PDV: a) – steel 12Kh18N10T; b) – magnesium Mg95

Conclusions

1. It was demonstrated that it is reasonable and effective to combine two techniques – PET and PDV in order to expand operability range, improve reliability and accuracy of sound velocities in shock-compressed structural and model materials.
2. Six explosive experiments were conducted with registration wave processes by combined technique PET-PDV. It was shown that in the field of relatively low stresses, PDV permits to register both velocity of interface "substance under study-indicator", and velocity of SW front that propagates over indicator. In the region of higher stresses and pressures, in indicator, SW front velocity is registered by PDV. This is complete analog of measurements conducted by PET, but with better accuracy.
3. Experimental-calculation determination was performed for longitudinal sound velocities for reference structural material – steel 12Kh18N10T and for model material – magnesium of Mg95 grade. The results obtained in each experiment by two independent techniques were compared in between and with the results obtained earlier. Their good agreement was shown.
4. Realization of proposed approach provides not only sufficient improvement of statistical representativity of the results of each experiment, but it is to take away contradictions, which exist for a long time in several important structural materials.

References

1. R.G.McQueen, J.W.Hopson, L.N.Fritz, Optical Technique for Determining Rarefaction Wave Velocities at Very High Pressures // Rev. Sci. Instr., 1982, V.53, No.2, pp.245-250.
2. E.A.Kozlov, V.I.Tarzhanov, D.G.Pankratov, A.K.Yakunin, V.M.Yelkin, V.N.Mikhaylov, Application of Optical Analyzer Technique for Measurements of Sound Velocities in Shock-Compressed Al-Mn Alloy for Calibration of Recent Elastic-Viscous-Plastic Models. Int. Conf. on High Energy Density Physics ZABABAKHIN SCIENTIFIC TALKS – 2005, Snezhinsk, Russia, September 5-10, 2005, Melville, New York, 2006, AIP Conference Proceedings, V.849, pp. 406-410.
3. E.A. Kozlov, D.G. Pankratov, O.V. Tkachyov, A.K. Yakunin, Sound velocity measurement in austenitic stainless steel 12KH18N10T in the range of stresses up to 200 GPA, International conference "Shock waves in condensed matter " (SWCM-2012), September 16-21, 2012, Kiev, Ukraine, pp.263-265.
4. E.A. Kozlov, D.G. Pankratov, O.V. Tkachyov, A.K.Yakunin, Sound Velocities and Shear Strength of Shocked U within 10-250 GPa, 19th European Conference on Fracture – Fracture Mechanics for

Durability, Reliability and Safety, August 26-31, 2012, Kazan, Russia, Book of Abstracts, p. 146, CD ROM, Paper No.603, 6 pages.
5. R.G.McQueen, J.M.Brown, Phase Transitions, Grüneisen Parameter, and Elasticity for Shocked Iron between 77 GPa and 400 GPa // J. of Geoph. Res., 1986, V.91, No.B7, pp. 7485-7494.
6. O.T.Strand, D.R.Goosman, C.Martinez, T.L.Whitworth, W.W.Kuhlow, A Novel System for High-Speed Velocimetry Using Heterodyne Techniques, Rev. Sci. Instrum. 77, 083108 (2006).
7. M.D.Bowden, M.P.Maisey, The development of a heterodyne velocimeter system for use in submicrosecond time regimes, Proc. of SPIE Vol. 6662, 66620B (2007);
8. J.Bénier, P.Mercier, E.Dubreuil, J.Veaux and P.A.Frugier, New heterodyne velocimeter and shock physics, DYMAT 2009, pp.289-294;
9. Shouxian Liu, Detian Wang, Tao Li, Guanghua Chen, Zeren Li, and Qixian Peng, Analysis of photonic Doppler velocimetry data based on the continuous wavelet transform, Rev. Sci. Instrum. 82, 023103 (2011).
10. E.A. Kozlov, S.A.Brichikov, D.P. Kuchko, M.A. Ralnikov, A.V.Olkhovsky, O.V.Tkachyov, The results of explosive experiments on acceleration of steel plates with simultaneous diagnostics of processes by two laser-interferometric techniques, Physics of burning & combustion, 2014 (in print).
11. E.A.Kozlov. Shock Adiabat Features, Phase Transition Macrokinetics, and Spall Fracture of Iron in Different Phase States. High Pressure Research. 1992, V.10, pp.541-582.
12. R.F.Trunin, L.F.Gudarenko, M.V.Zhernokletov, G.V.Simakov. Experimental data on shock-wave compression and adiabatic expansion of condensed matters // Sarov: RFNC-VNIIEF, 2001, p. 446.
13. M.F.gogulya, A.K.Yakunin, Radiation of shock-compressed methane halogen derivatives // Physics of burning & combustion, 1988, V.24, No.6, pp.127-134.
14. L.F.Gudarenko, M.V.Zhernokletov, S.I.Kirshanov, A.E.Kovalev, V.G.Kudelkin, T.S.Lebedeva, A.I.Lomaikin, M.A.Mochalov, G.V.Simakov, A.N.Shuikin, I.M.Voskoboinikov. Experimental investigations into the properties of shock-compressed carbogal. EOS of carbogal and organic glass. Physics of burning & combustion, 2004, V.40, No.3, pp.104-116.
15. G.V.Sin'ko and N.A.Smirnov, *Ab initio* calculations for the elastic properties of magnesium under pressure // Phys. Rev. B, V.80, 2009, c.104113.
16. V.M.Elkin, V.N.Mikhailov, T.Yu.Mikhailova, Semi-empirical models of shear modulus in a wide range of temperatures and pressures of shock compression, Physics of burning & combustion, 2011, V.112, No.6, pp.563-576
17. J.W.Shaner, R.S.Hixson, D.A.Boness, Birch's Law for Fluid Metals // In: Shock Waves in Condenced Matter – 1987, Elsevier Science Publisher, B.V., pp.135-138.
18. E.A. Kozlov, D.G. Pankratov, A.K.Yakunin, A.G.Poptsov Sound velocity measurement in shock-compressed magnesium alloy MA-14, XV International conference Khariton scientific readings, March 18-22, 2012, Sarov, Russia.

ИЗМЕРЕНИЕ КИНЕМАТИЧЕСКИХ И ТЕПЛОВЫХ ХАРАКТЕРИСТИК БЫСТРОПРОТЕКАЮЩИХ ГАЗОДИНАМИЧЕСКИХ ПРОЦЕССОВ С ПОМОЩЬЮ КОМПЛЕКСА МИКРОВОЛНОВОГО ЗОНДИРОВАНИЯ

Е.В. Ботов[2], В.Н. Иконников[3], В.А. Канаков[3], Н.С. Корнев[1], К.В. Минеев[1], А.В. Назаров[1], А.А. Седов[2]

[1]ФНПЦ НИИИС им. Ю.Е. Седакова, Нижний Новгород, Россия
[2]РФЯЦ-ВНИИЭФ, Саров, Россия
[3]Нижегородский государственный университет им. Н.И. Лобачевского, Нижний Новгород, Россия

Измерение параметров быстропротекающих газодинамических процессов является актуальной задачей для предприятий, занимающихся разработкой взрывчатых составов. Методики